

54#
~~CONFIDENTIAL~~
~~UNCLASSIFIED~~
~~CONFIDENTIAL~~

5451 5411k
30-21

~~M. L. Musselman~~

NRL Report 4537

Copy No. 60

UNCLASSIFIED

FIELD PATTERNS OF HORIZONTAL-WIRE ANTENNAS SUBMERGED IN SEAWATER

~~CONFIDENTIAL~~
UNCLASSIFIED SECRET TITLE

M. L. Musselman and G. W. Roos

Communication Branch
Radio Division

~~CONFIDENTIAL~~
~~UNCLASSIFIED~~
~~CONFIDENTIAL~~

May 25, 1955

~~CONFIDENTIAL~~
~~UNCLASSIFIED~~
~~CONFIDENTIAL~~

1221-100:FW:ST
22 Feb 1982

APPROVED FOR PUBLIC RELEASE
DISTRIBUTION UNLIMITED



~~CONFIDENTIAL~~
~~UNCLASSIFIED~~
~~CONFIDENTIAL~~

~~CONFIDENTIAL~~
~~UNCLASSIFIED~~
~~CONFIDENTIAL~~
~~UNCLASSIFIED~~
~~CONFIDENTIAL~~

NAVAL RESEARCH LABORATORY
Washington, D.C.

GROUP-3
Downgraded at 10 year intervals;
Not automatically declassified.

SECRET

SECURITY

This document contains information affecting the national defense of the United States within the meaning of the Espionage Laws, Title 18, U.S.C., Sections 793 and 794. The transmission or revelation of its contents in any manner to an unauthorized person is prohibited by law.

Reproduction of this document in whole or in part is prohibited except with permission of the issuing office.

SECRET

~~SECRET~~

~~UNCLASSIFIED~~
ABSTRACT

[Secret]

Scale-model experiments were conducted to determine the radiation pattern in air above horizontal insulated-wire antennas submerged in seawater. Radiation patterns were measured over a wide range of frequencies for both end-exposed and end-sealed antennas that varied in physical lengths from 2 to 16 feet. Antenna cables with ratios of dielectric diameter to conductor diameter of 3.6 and 11.2 were used for the measurements.

The results showed that the radiation pattern in air was a figure eight for all antennas of electric length less than $1/4$ wavelength. The major lobes of the pattern were axial to the antenna. As the antenna length was increased to $3/4$ wavelength, the lobes of the figure-eight pattern began to split with reduced field strength in the direction of the antenna. The ratio of dielectric diameter to conductor diameter did not affect the shape of the patterns. The change or split in the lobes of a figure-eight pattern is explained in terms of the phase angle introduced by the difference in propagation constants between air and the antenna dielectric. These results applied to both end-exposed and end-sealed antennas.

PROBLEM STATUS

This is an interim report; work on the problem is continuing.

AUTHORIZATION

NRL Problem R01-06
Project Nos. NR 681-060 and
NE 121-021, 17, 18, and 19
BuShips Problem S-1510

Manuscript submitted April 12, 1955

~~SECRET~~

~~SECRET~~

UNCLASSIFIED

FIELD PATTERNS OF HORIZONTAL-WIRE ANTENNAS SUBMERGED IN SEAWATER

INTRODUCTION

Studies of electromagnetic wave propagation in salt water show that to establish radio communications between completely submerged locations will require an antenna unique in its physical and electrical characteristics (1). The analysis of the composite propagation path of seawater and air at frequencies in the vlf range has shown the horizontal insulated-wire antenna to have many essential properties for a submerged radiator. This antenna has been investigated to determine the parameters for optimum design.

The insulated-wire antenna is simply a copper conductor encased in a dielectrical material and submerged in salt water in a horizontal position. Two types of antenna can be constructed, the end-exposed and the end-sealed type. The end-exposed antenna has the conductor at the far end exposed for a sufficient length to insure adequate contact with the seawater. In the end-sealed antenna, the inner conductor is insulated from the seawater by dielectric material over its entire length.

Theoretical expressions for input impedance of the two types of antennas have been developed, and were verified by experiments conducted on a scaled-model basis (2). The values of impedance for antennas of practical dimensions were such as to represent a good load for either receiver or transmitter equipment. In choosing between the two types of antennas on an impedance basis, the end-exposed antenna is the better since short lengths have an inductive impedance, which simplifies the problem of obtaining a good match to the equipment.

The radiation and reception properties of the horizontal-wire antennas have also been expressed by theoretical formulas and these have also been substantiated by scale-model measurements (3). The results showed that the inducted voltage for reception, or the radiated field for transmission, increased with increasing antenna length. Maximum values were reached at $1/4$ wavelength and $1/2$ wavelength for the end-exposed and end-sealed antennas respectively. It was also shown that end-exposed antennas as short as $1/10$ wavelength were still efficient radiators, indicating low loss resistance. The end-sealed antenna of this short length was inefficient. Since practical application would require the antenna to be short in physical length, the end-exposed type would again be the better antenna.

To complete the analysis of the submerged horizontal insulated-wire antenna, a series of experiments was conducted to determine the radiation field pattern in air and the factors influencing the pattern. These measurements were made on a scaled-model basis.

THEORY

A submerged insulated horizontal-wire antenna radiates in a manner fundamentally similar to that of an antenna in air, with a field pattern in the water essentially omnidirectional. The attenuation of the radiated energy as it is propagated through the water is an exponential function of the distance traveled. This rapid increase in attenuation limits, for all practical purposes, the range that can be achieved through a seawater path

~~SECRET~~

~~UNCLASSIFIED~~

SECRET
UNCLASSIFIED

to less than 100 feet. However, a wave front lying within about one degree of normal to the surface penetrates the seawater-air boundary and propagates into the air. This phenomenon provides the only means of obtaining radio communications over an extended range. The antenna must be submerged to depths not greater than 10 feet since the attenuation in the water would become excessive. Two distinct radiation patterns therefore exist for a submerged antenna; one occurs totally in the water medium, and the second is produced by the field penetrating the interface. Since the seawater-air propagation path is that used to obtain an extended range for the system, the pattern in air is the more significant and is normally the one considered in defining the pattern of a submerged antenna.

The part of a wave front that penetrates the seawater-air boundary spreads out or diverges from an angle of one degree width in the seawater to nearly 180 degrees in air. The ratio of the energy density in air to that in water is defined as the refraction coefficient (1). Refraction at the surface produces a change in the polarization of a wave which has an influence on the pattern.

In considering the polarization effects on a pattern, the area over which the pattern will be determined must be specified. The system considered here is concerned with only that portion of the refracted energy which has its propagation path directed along the surface. In practice this means the reception point would be located either on or beneath the surface, rather than high above the surface. The pattern for this condition corresponds to the horizontal pattern for antennas in air.

A radio wave emanating from a submerged horizontal-wire antenna is polarized in the plane of the antenna. The part of this wave that propagates along an underwater path nearly normal to the surface and then along the surface in air has a change in the direction of propagation of nearly 90 degrees. There must also be a corresponding change in the plane of polarization. Since the initial field in the seawater has the E vector in the direction of the antenna, then the field that is refracted broadside to the antenna would be horizontally polarized. The field that is refracted along the axis of the antenna would be vertically polarized. Thus, the field strength pattern in air along the surface for the vertically polarized wave would have a figure eight shape with the maxima in the direction coaxial to the antenna. Vertically polarized elements of the wave front are of practical importance since they propagate at the seawater surface with normal inverse distance attenuation while the horizontally polarized wave attenuates more rapidly.

The total field at a distant point in air is composed of a vector summation of wave elements emanating from the total length of the antenna. Each of these wave elements travels a slightly different path, causing a phase shift in the vector summation at the reception point. This can be explained by Fig. 1 which shows that energy from point (A) travels a very short distance along the antenna before it penetrates the surface where it propagates in air the distance (r) before reaching (P), the point of reception. Energy from point (B) travels the full length of the antenna (ℓ), before it penetrates the surface where it propagates in air the distance (r') before reaching (P). The distance (d) that each wave travels through the water is equal, and therefore, can be eliminated from this analysis. The propagation constant for the antenna path differs from that in air by about 3 to 1. This difference produces a phase shift which can be expressed as:

$$\Phi = \ell - D, \quad (1)$$

SECRET

where

Φ = phase shift

l = electrical length of antenna in seawater

D = electrical length of the difference in paths in air.

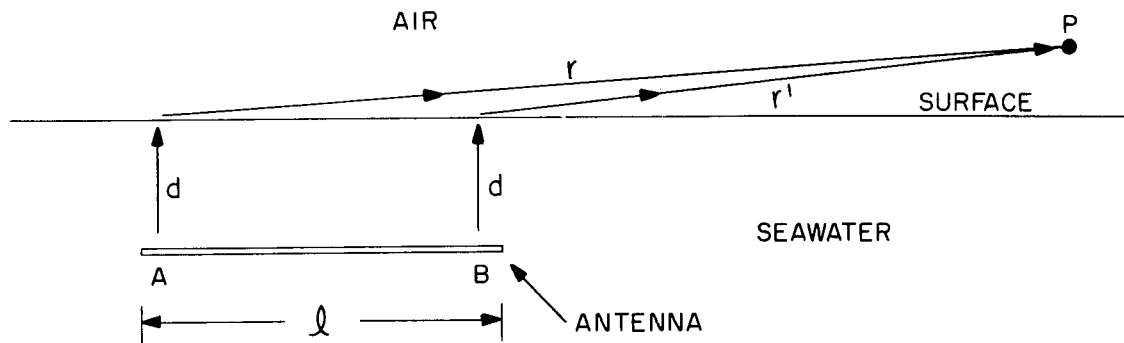


Fig. 1 - Schematic showing difference in propagation path

As seen by Eq. (1), the magnitude of the phase shift is dependent on the antenna length. Electrical lengths of $1/4$ wavelength or less produce a small phase shift which will not alter the figure eight pattern. For antenna lengths greater than $1/4$ wavelength the phase shift in the vector summation becomes important, reaching 180 degrees at points coaxial with the antenna for an antenna length of $3/4$ wavelength. Thus, as the antenna length approaches $3/4$ wavelength a split occurs in the lobes of the figure-eight pattern with a minimum field strength axial to the antenna.

The two factors, therefore, that influence the horizontal radiation pattern in air of a submerged insulated-wire antenna are the refraction at the surface and the phase shift between the air and antenna path. These factors apply equally to end-exposed or end-sealed antennas. Although this discussion has been based on waves emanating from submerged transmitting antennas, it can be shown that identical patterns exist in air for submerged receiving antennas with a plane wave propagating over the surface.

EXPERIMENTAL MEASUREMENTS

Measurements were made to obtain experimental data on the horizontal radiation patterns in air for submerged insulated-wire antennas. To provide controlled conditions and simplicity in techniques, the experiments were made on a scaled-model basis. An area to the south of the Naval Research Laboratory was selected as the site for the model range.

SECRET
UNCLASSIFIED

Installation

An isometric drawing of the model-range installation is shown in Fig. 2. Two tanks (one 18 feet long, 30 inches wide, and 16 inches deep; the second 8 feet long, 30 inches wide, and 16 inches deep) were included. A solution of ammonium chloride which produced a conductivity of 50 mhos per meter was contained in the tanks. Inasmuch as the conductivity of seawater averages about 4 mhos per meter, the scaling factor of the model range was approximately 12 to 1. A wire-mesh screen was employed to provide a continuous ground path between the solution in the tanks and ground. Shielded cubicles were located at the end of each tank as a place for measurement equipment. A detailed description of the model range can be found in Ref. (1).

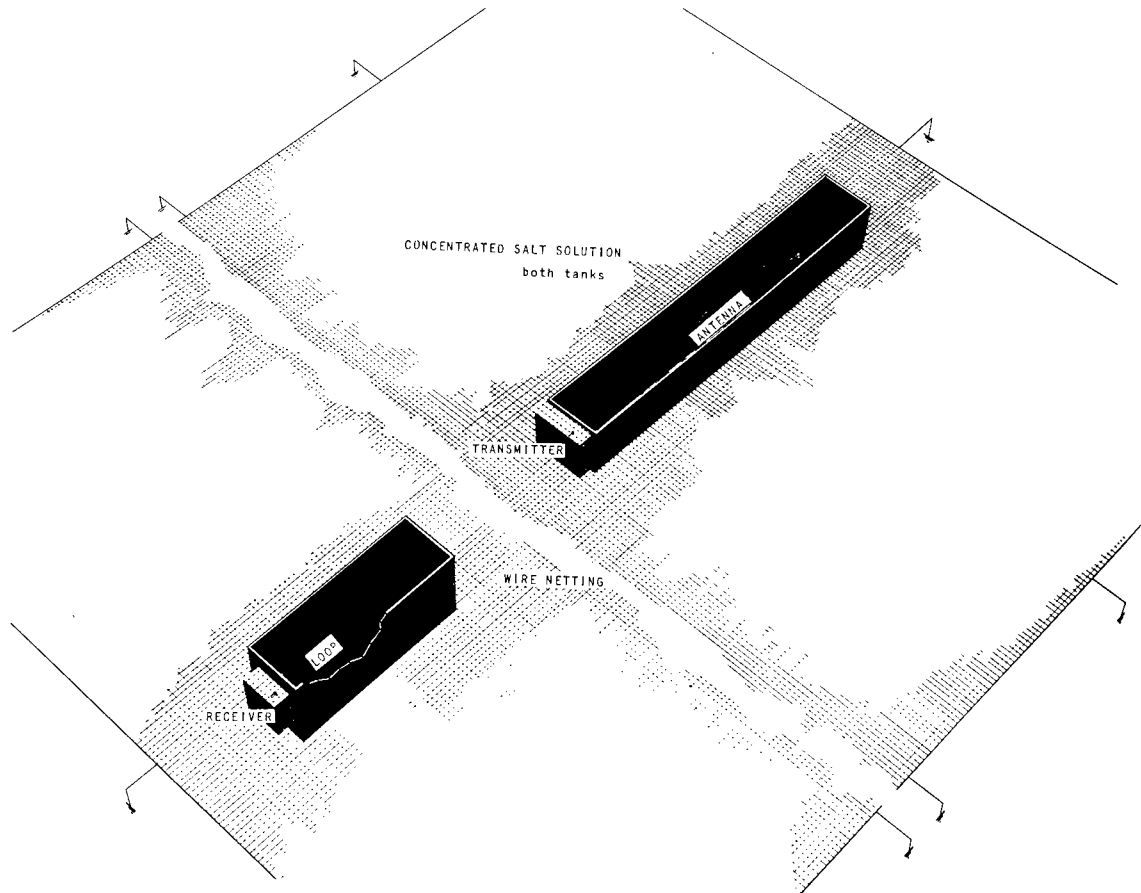


Fig. 2 - Isometric drawing of scaled-model range

A Navy Model TDE transmitter was installed in the shielded cubicle at the 18-foot tank. A short tube between the cubicle and the tank provided a shielded path for feed lines to connect to the antenna.

Measurements in air of absolute field strength were made with an RCA 308-B field-strength meter. An Electronic Instrument Corp. portable field-strength meter was used to measure relative field strength.

SECRET

Scaled-Model Antennas

Radiation patterns from a submerged insulated-wire antenna were measured, over a frequency range, for various antenna lengths and for various ratios of over-all antenna diameter to conductor diameter. The antenna length was varied in steps of 2 feet, from 16 to 2 feet for the end-exposed antenna and from 16 to 4 feet for the end-sealed antenna. These lengths correspond to full-scale antennas varying in length from 192 to 24 feet. Antennas of lengths less than this are inefficient because of a predominant loss resistance.

To obtain a variation in the ratio of the over-all diameter to the conductor diameter, three different antennas were selected. The three antenna cables were made by stripping back the vinyl covering and copper shield of RG-58/U, RG-5/U, and RG-63/U coaxial transmission lines for the desired length. The physical constants of these three antenna cables are listed in Table 1. The antennas selected for these experiments had sufficient range in the ratio of over-all diameter to conductor diameter so that the significances of the dielectric thickness could be determined.

TABLE 1
Dielectric and Conductor Diameters for
the Various Antennas

Type of Antenna	Conductor Diameter (in.)	Over-All Diameter (in.)	Ratio
RG-5/U	0.0508	0.185	3.64
RG-58/U	0.0320	0.116	3.63
RG-63/U	0.0254	0.285	11.20

A four-foot section of transmission line of the same type as that from which the respective antennas were formed, and continuous with the antenna, was used as the feed line. The outer conductor of the four-foot section was carefully grounded to the salt solution to provide ground return.

Measurement Procedure

Measurements of three quantities were necessary to obtain the desired information about the horizontal pattern in air from a submerged antenna. These quantities are: (1) the input impedance of the submerged transmitting antenna, (2) the current feed into the transmitting antenna, and (3) the horizontal pattern of the field in air around the antenna. Measurements of these quantities were made at frequencies of 1, 2, 4, 6, 8, and 10 Mc using the three antennas described in the previous section, both end-exposed and end-sealed. Since variation in the depth of an antenna does not affect the pattern in air, all measurements were made at a fixed depth of 1 inch.

The Navy Model TDE transmitter supplied energy to the antenna through the 4-foot transmission line. When necessary, a series capacitor was used to permit proper loading to the antenna. The r-f current into the 4-foot feed line was measured with calibrated ammeters.

The input impedance was measured with a standard r-f bridge, General Radio Model 916-A. These measurements were made at the transmitter end of the feed line, the point at which the current was measured. Power input was then calculated from the known current and input resistance.

Field intensity measurements of the vertically polarized wave were made on a circular path of 200-foot radius with the center at the mid-point of the antenna. The RCA 308-B meter was used to obtain absolute values of field strength axial to the antenna. The Electronic Instruments Corporation portable field intensity meter was used to obtain relative values of field strength at fixed points along the circular path. These readings were converted to absolute values based on the data recorded by the 308-B. Field strengths were measured for only one fourth of the circular path since, by symmetry of pattern, the data obtained in the remaining three quadrants would be identical. Measurements were made at 0, 22, 45, 67, and 90 degrees at 200 feet.

Data and Results

The measured data of impedance, antenna r-f current and absolute field strength at the 0-degree position are presented in Tables 2, 3, and 4 for RG-5/U, RG-58/U, and RG-63/U antennas respectively. The power as calculated from the antenna current and resistance is also shown in the three tables. Measurement difficulties caused by extreme impedance values blocked efforts to obtain data under certain conditions corresponding to the blank portions of the tables.

Before the absolute field strength values shown in the tables could be used to calculate the field patterns these had to be standardized to constant power for each measurement. One hundred watts was chosen arbitrarily as the standard and all data were corrected accordingly.

Attenuation for a given depth and refraction at the interface are functions of frequency (1). In order to analyze the pattern data only for effects caused by the antenna and propagation conditions, the frequency effects of attenuation and refraction were calculated and eliminated. It should be noted in the pattern graphs that the magnitude of the field intensity is changed from microvolts per meter to volts per meter.

Another factor to consider is the effect of measuring current and impedance at the end of the 4-foot feedline rather than directly at the antenna. Since the measurement frequencies were 10 Mc or below and the line length involved was short, a correction was made only for the action of the line as a perfect transformer.

On the basis of the corrected value of absolute field strength at the 0-degree position, field patterns were calculated from the relative values measured by the Instruments Corporation meter. In Appendix A, Figs. 3A to 22A, the corrected pattern data is shown in polar plot at the various frequencies for which each antenna was measured.

A figure-eight radiation pattern was measured for all antennas of electrical length less than $1/4$ wavelength, either end-exposed or end-sealed. The ratio of the inner-conductor diameter to the over-all diameter did not significantly alter the shape of the pattern. The level of field intensity is a function of the antenna radiation efficiency (3). This factor proportionately reduces the pattern but does not appreciably change the shape.

TABLE 2
Measured Impedance, Current, and Field Strength Data for RG-5/U Antennas

Frequency (Mc)	Antenna Length (feet)	End-Exposed				End-Sealed			
		Impedance (ohms)	Current (amps)	Power (watts)	Field Strength* (μ volts/meter)	Impedance (ohms)	Current (amps)	Power (watts)	Field Strength* (μ volts/meter)
1	16	7.0-j34	2.6	47	230	2.0-j150	3.6	26	123
2		18.4+j73	3.0	166	820	4.2-j75	6.6	183	600
4		312.0+j225	---	---	---	6.2-j23	4.6	131	690
6		41.5-j133	1.6	106	1430	16.0+j11	3.4	185	1200
8		13.0-j63	---	---	---	54.0+j61	2.0	216	1485
10	12.4-j23	3.4	143	490	190.0-j20	---	---	---	
1	12	5.8+j25	3.0	52	195	2.0-j400	---	---	---
2		12.0+j52	3.6	156	635	2.5-j200	---	---	---
4		57.5+j131	2.0	230	1190	4.4-j63	5.0	110	670
6		385.0-j150	---	---	---	7.6-j33	4.4	147	1030
8		45.5-j125	2.0	182	1460	16.3+j14	---	---	---
10	16.5-j70	3.2	174	1100	42.5+j51	2.0	170	1780	
1	8	3.8+j18	3.35	43	140	---	---	---	---
2		7.8+j34	4.2	137	475	1.0-j280	---	---	---
4		21.0+j73	3.0	189	750	1.5-j100	6.0	54	360
6		81.0+j148	1.6	207	1090	2.8-j67	5.8	94	610
8		405.0-j25	---	---	---	5.7-j25	5.2	154	930
10	83.0-j163	1.2	120	1245	8.4-j3	4.5	170	860	
1	4	2.2+j10	3.0	20	62	0.3-j700	---	---	---
2		4.2+j20	5.0	105	330	0.5-j350	---	---	---
4		8.0+j38	4.4	155	725	0.7-j175	7.6	40	205
6		15.8+j60	3.2	161	890	0.9-j108	6.3	36	285
8		32.0+j91	2.4	161	845	1.2-j75	6.5	51	365
10	89.0+j155	---	---	---	1.7-j50	7.2	88	565	
2	2	2.0+j11	5.6	63	171	---	---	---	---
4		4.0+j23	5.5	121	410	---	---	---	---
6		6.3+j36	4.0	101	450	---	---	---	---
8		9.6+j49	4.0	154	585	---	---	---	---

*Field strength measured with 308-B meter at 0-degree position

TABLE 3
Measured Impedance, Current, and Field Strength Data for RG-58/U Antennas

Frequency (Mc)	Antenna Length (feet)	End-Exposed			End-Sealed			
		Impedance (ohms)	Current (amps)	Power (watts)	Field Strength* (μ volts/meter)	Impedance (ohms)	Current Power (amps) (watts)	Field Strength* (μ volts/meter)
1	16	7.6+j37	3.0	68	245	---	---	---
2		19.8+j78	2.6	134	660	3.5-j190	5.0	88
4		---	---	---	---	7.4-j50	4.2	131
6		52.0-j158	1.6	133	1380	18.9+j19	2.0	76
8		16.6-j69	3.0	149	670	74.0+j18	1.0	74
10		16.2-j24	3.0	146	630	---	---	---
1	12	6.0+j27	3.0	54	170	---	---	---
2		12.5+j55	3.4	145	630	2.2-j150	5.0	55
4		66.0+j150	1.5	148	1020	4.3-j58	4.6	91
6		---	---	---	---	8.4-j16.7	4.0	134
8		39.5-j131	2.0	158	1150	17.7+j21	2.4	102
10		15.9-j70	2.0	64	545	53.0+j70	1.8	172
1	8	4.4+j19	3.2	45	125	---	---	---
2		7.8+j37	4.4	151	560	---	---	---
4		23.0+j83	3.0	207	1020	2.4-j113	---	---

*Field strength measured with 308-B meter at 0-degree position

TABLE 4
Measured Impedance, Current, and Field Strength Data for RG-63/U Antennas

Frequency (Mc)	Antenna Length (feet)	End-Exposed				End-Sealed			
		Impedance (ohms)	Current (amps)	Power (watts)	Field Strength* (μvolts/meter)	Impedance (ohms)	Current (amps)	Power (watts)	Field Strength* (μvolts/meter)
1	16	7.8+j40	2.8	61	280	1.5-j800	---	---	---
2		17.5+j78	3.2	179	755	2.7-j375	---	---	---
4		---	---	---	---	5.6-j175	4.1	94	935
6		256.0+j417	0.95	244	2280	9.5-j83	3.8	137	1420
8		460.0-j103	---	---	---	17.0+j0	3.2	174	1270
10		69.0-j240	1.5	155	1400	---	---	---	---
2	12	10.8+j60	3.3	118	495	5.0-j250	3.5	61	200
4		36.0+j135	2.0	144	790	7.5-j75	4.0	120	470
8		182.0-j225	0.9	147	1620	18.5+j51	3.0	167	1180
2	8	7.0+j40	4.0	112	340	2.4-j600	---	---	---
4		14.0+j77	3.2	144	555	1.9-j300	---	---	---
8		52.0+j200	1.7	150	590	3.5-j125	4.0	56	465
2	4	3.9+j24	4.6	83	185	2.0-j925	---	---	---
4		7.0+j46	4.4	136	350	1.0-j450	---	---	---
8		15.7+j94	3.0	141	375	1.2-j213	---	---	---

*Field strength measured with 308-B meter at 0-degree position

For frequencies at which the electrical length of the antenna exceeded $1/4$ wavelength, patterns were found to have a minimum axial with the antenna. These results are shown in Appendix A, Figs. A-3, A-4, A-9, A-12, and A-17. In each case the antenna length was approaching $1/2$ wavelength, indicating that at this length the phase angle defined in the theory section had become sufficiently large to influence the pattern. The scaled-model range was not designed to permit measurements of $3/4$ -wavelength antennas for determining maximum effect of phase angle. The data presented, however, are sufficient to verify the existence of the phase-angle effect and to predict the resultant pattern.

CONCLUSIONS

For the vertically polarized wave in air, a figure-eight radiation pattern exists for all submerged horizontal insulated-wire antennas if the length is no greater than $1/4$ wavelength. For frequencies or antenna physical lengths such that the electrical length of the antenna is $1/2$ wavelength or longer, the single lobes of the figure-eight pattern start to split, resulting in reduced field strength in the direction of the antenna. Since a figure-eight pattern represents gain in the direction coaxial with the antenna, the antenna length in practice should not exceed $1/4$ wavelength.

* * *

REFERENCES

1. Norgorden, O., "The Submerged Reception of Radio Frequency Signals," NRL Report R-1669 (Unclassified), December 2, 1940
2. Flath, E. H., Jr., and Norgorden, O., "Expressions for Input Impedance and Power Dissipation in Lossy Concentric Lines," NRL Report R-3436 (Unclassified), March 24, 1949; Appleman, C. B., "Impedance of Submerged Horizontal-Wire Antennas," NRL Report 3889 (Secret), December 20, 1951
3. Musselman, M. L., "Reception with Submerged Horizontal-Wire Antennas," NRL Report 4180 (Secret), September 10, 1953; Rauen, T. J., "Submerged Horizontal-Wire Transmitting Antennas," NRL Report 4250 (Secret), November 5, 1953
4. Musselman, M. L., "Key West Experiments on Horizontal-Wire Antennas," NRL Report 3841 (Secret), August 6, 1951

* * *

APPENDIX A Antenna Radiation Patterns

Figures A-1 through A-20 show the horizontal radiation patterns of submerged horizontal insulated-wire antennas as the patterns would appear in air above the antennas. These patterns show the effect of variations in frequency, antenna length, and ratio of over-all antenna diameter to conductor diameter. The data have been corrected for the frequency effect of the conducting medium. All results were obtained on a scaled-model basis.

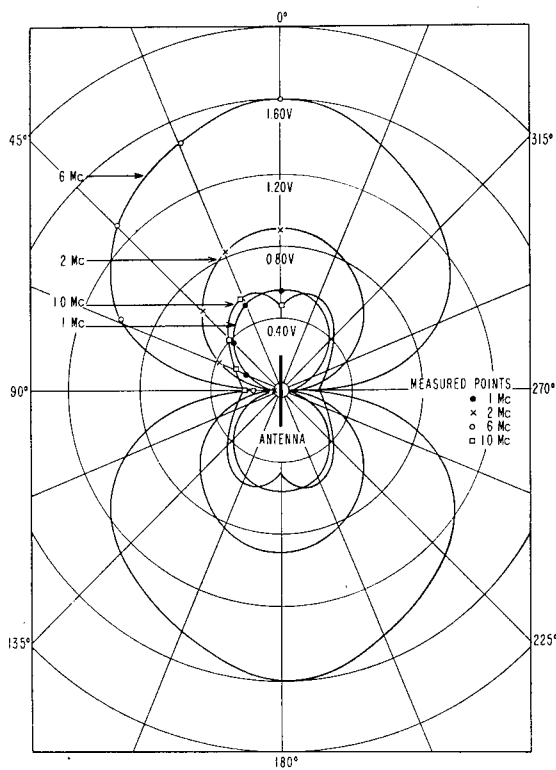


Fig. A-1. Sixteen-Foot End-Exposed
RG-5/U

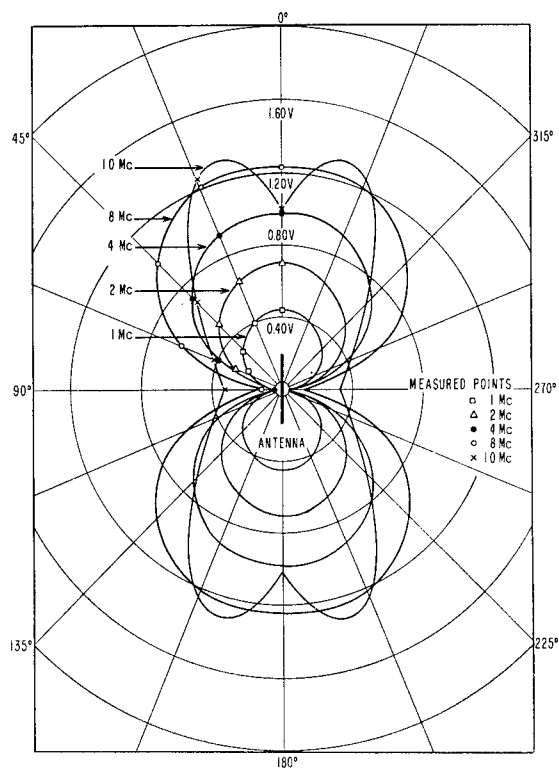


Fig. A-2. Twelve-Foot End-Exposed
RG-5/U

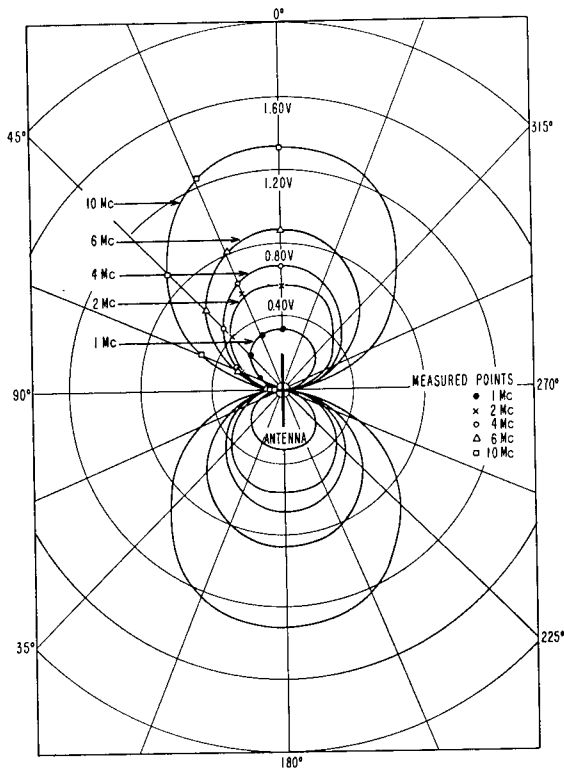
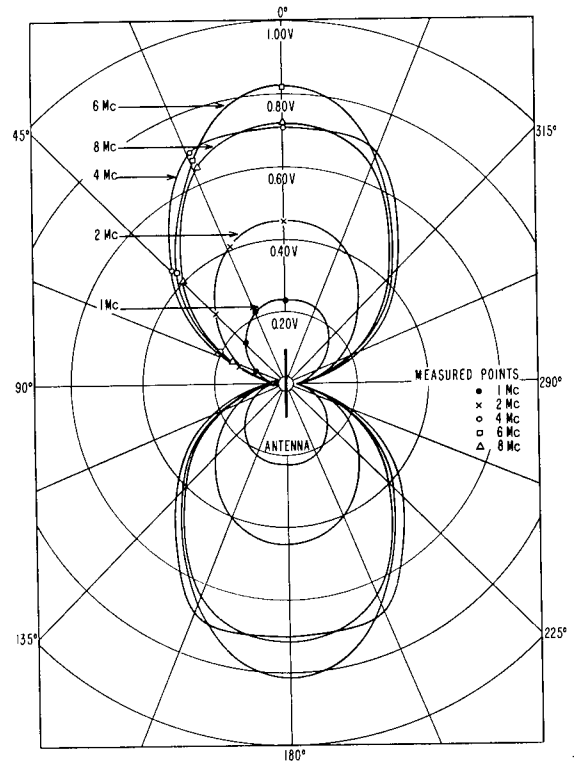


Fig. A-4. Four-Foot End-Exposed RG-5/U

Fig. A-3. Eight-Foot End-Exposed RG-5/U



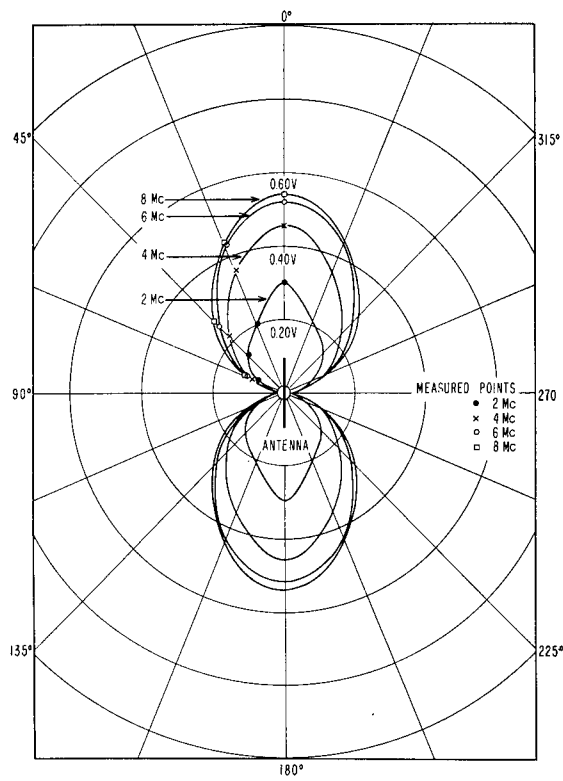


Fig. A-5. Two-Foot End-Exposed
RG-5/U

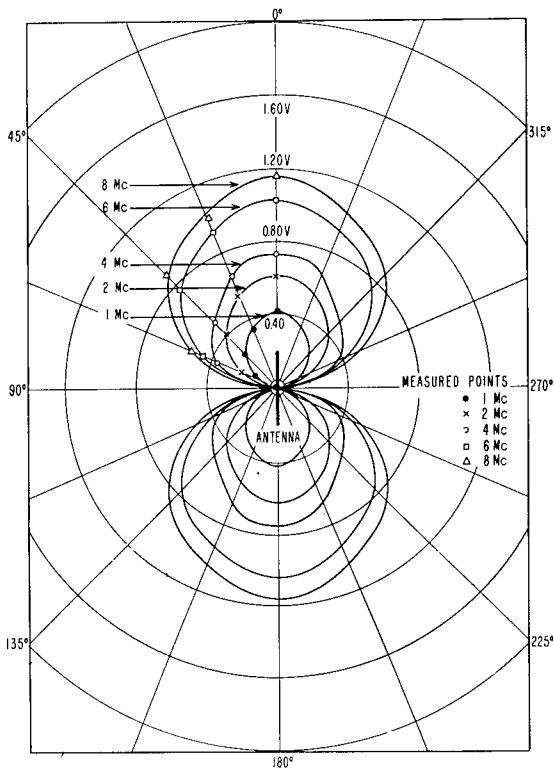


Fig. A-6. Sixteen-Foot End-Sealed RG-5/U

Fig. A-7. Twelve-Foot End-Sealed RG-5/U

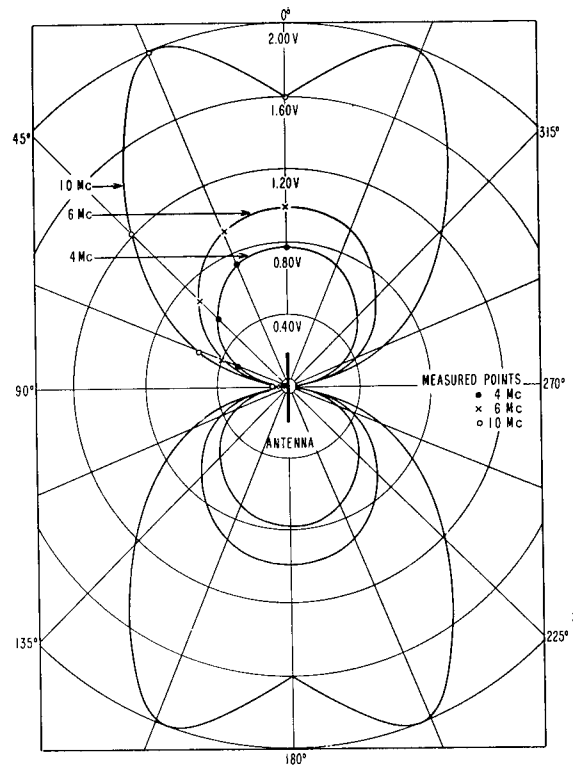


Fig. A-8. Eight-Foot End-Sealed
RG-5/U

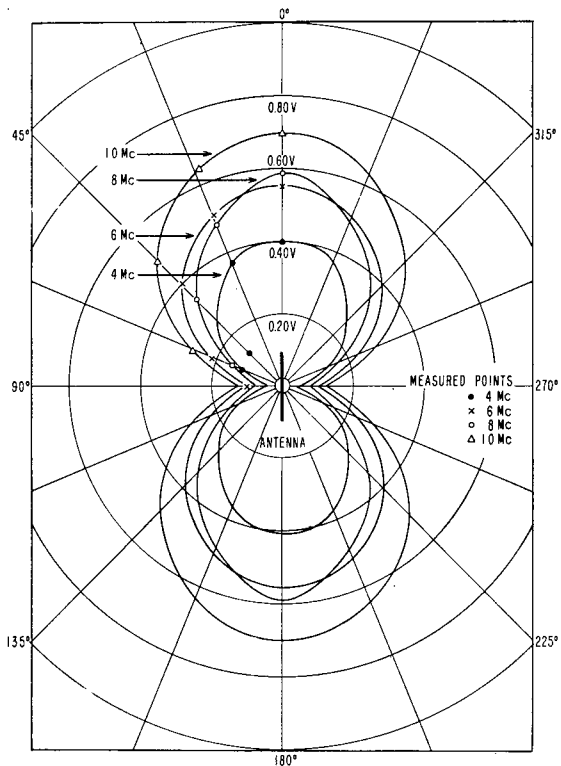
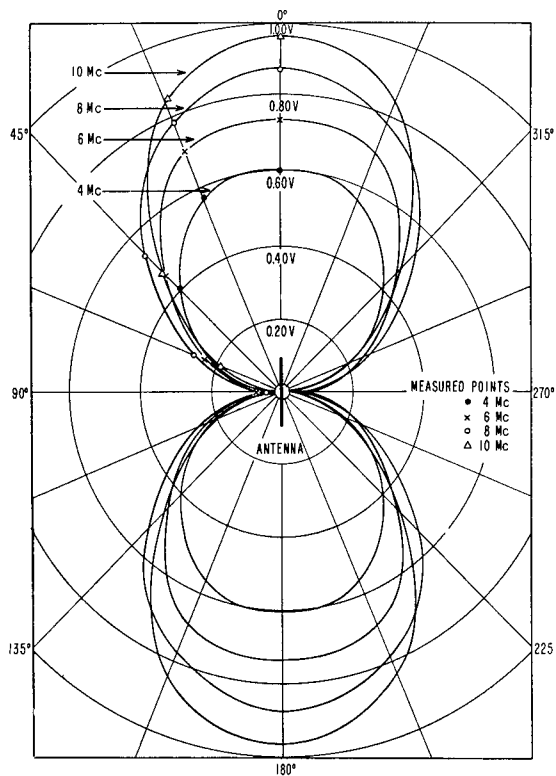


Fig. A-9. Four-Foot End-Sealed
RG-5/U

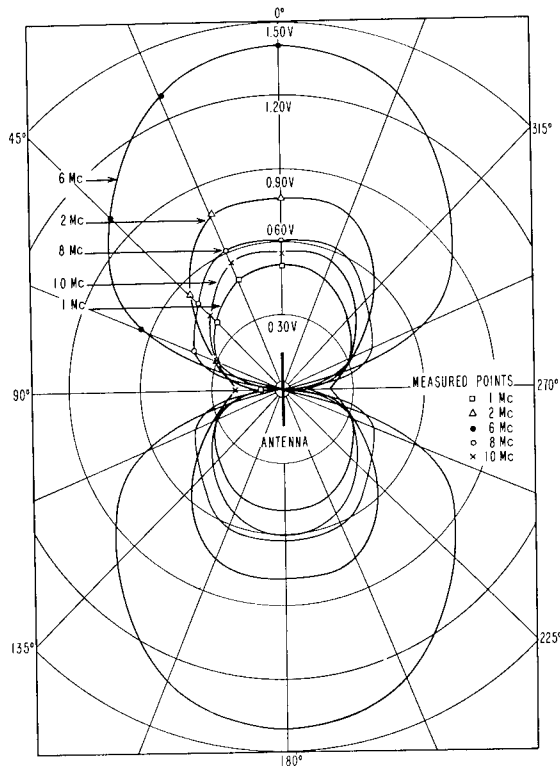
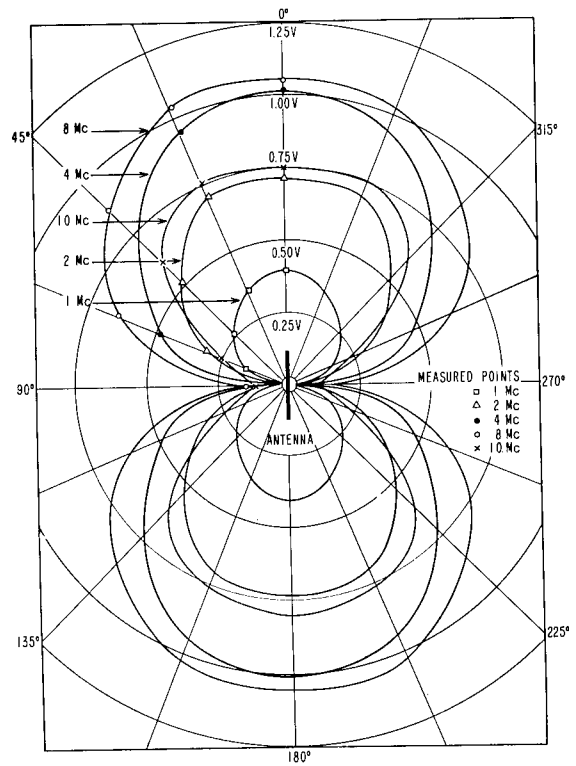


Fig. A-10. Sixteen-Foot End-Exposed RG-58/U

Fig. A-11. Twelve-Foot End-Exposed RG-58/U



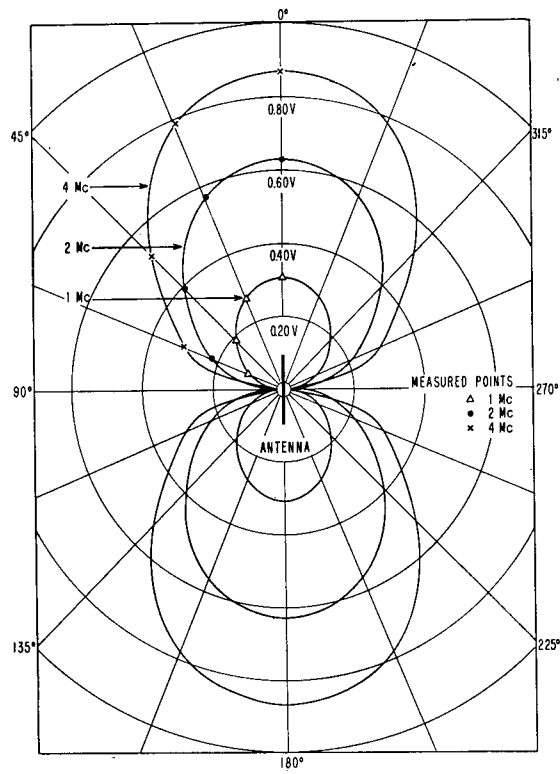


Fig. A-12. Eight-Foot End-Exposed
RG-58/U

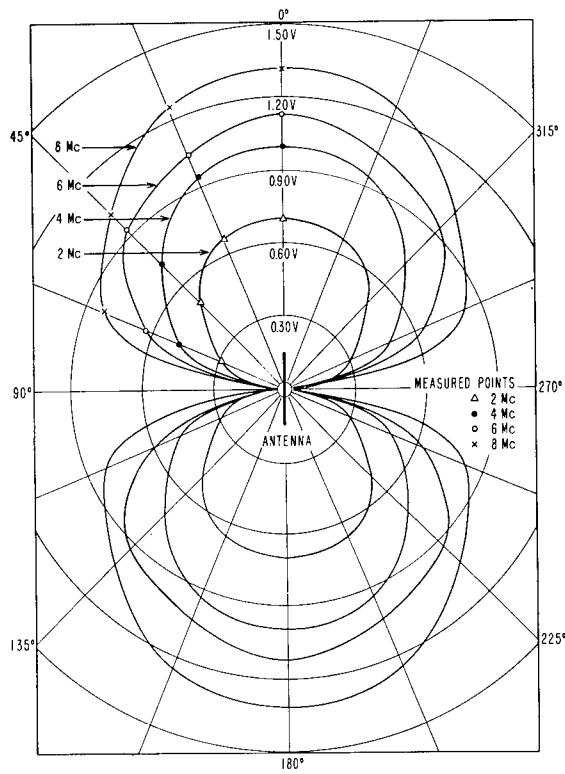


Fig. A-13. Sixteen-Foot End-Sealed RG-58/U

Fig. A-14. Twelve-Foot End-Sealed RG-58/U

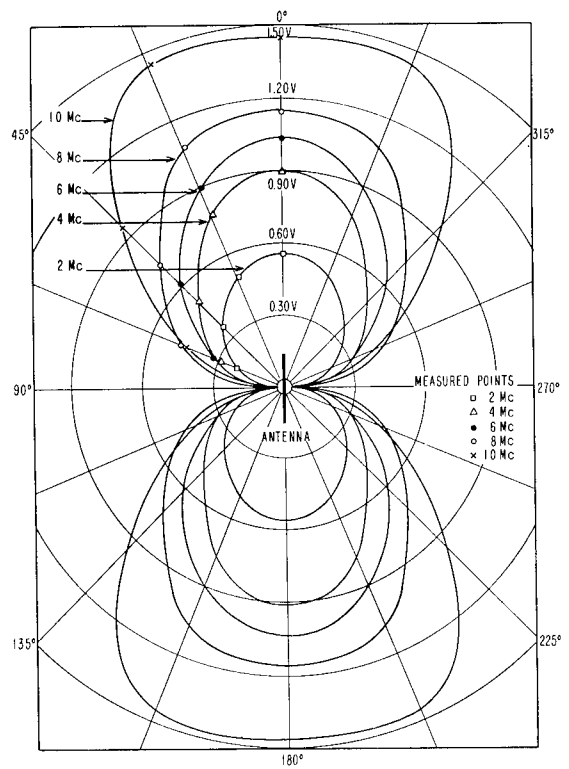


Fig. 15-A. Sixteen-Foot End-Exposed RG-63/U

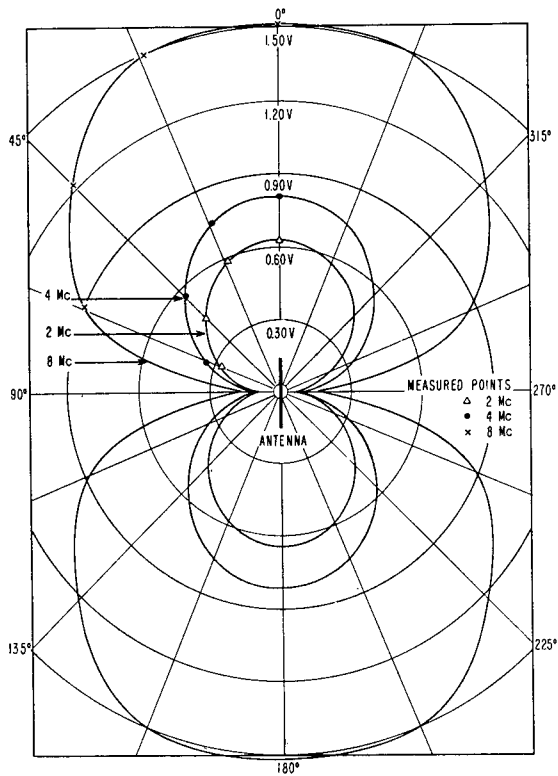
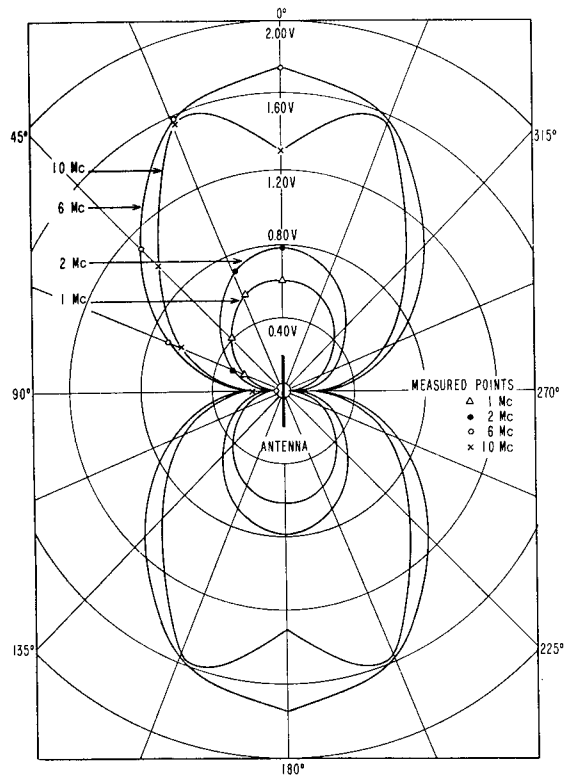


Fig. A-16. Twelve-Foot End-Exposed RG-63/U

~~SECRET~~

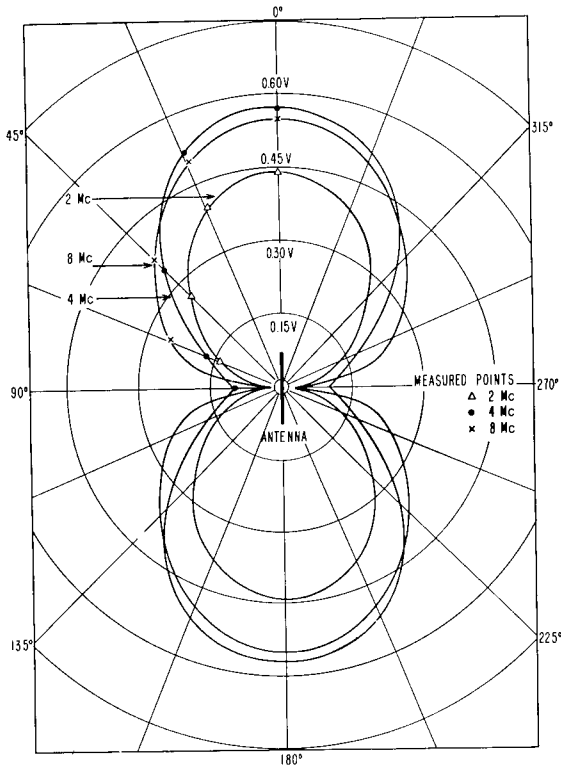
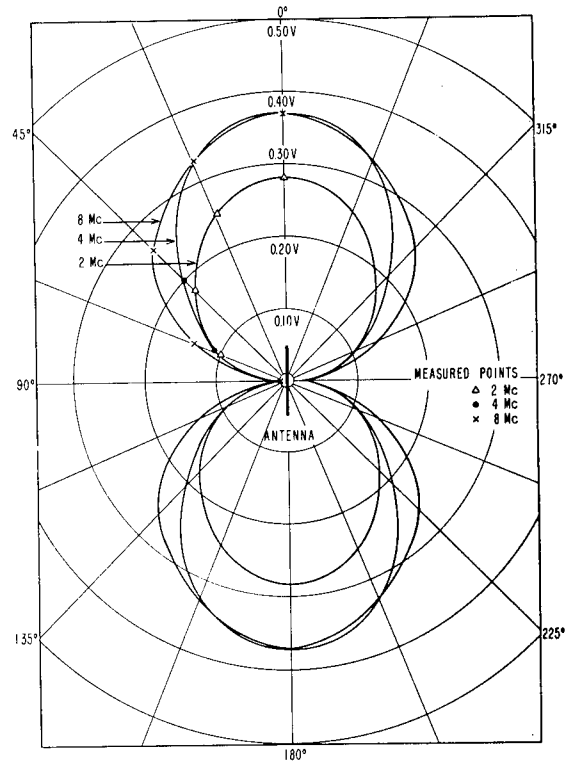


Fig. A-17. Eight-Foot End-Exposed RG-63/U

Fig. A-18. Four-Foot End-Exposed RG-63/U



SECRET

SECRET
UNCLASSIFIED

UNCLASSIFIED

Fig. A-19. Sixteen-Foot End-Sealed RG-63/U

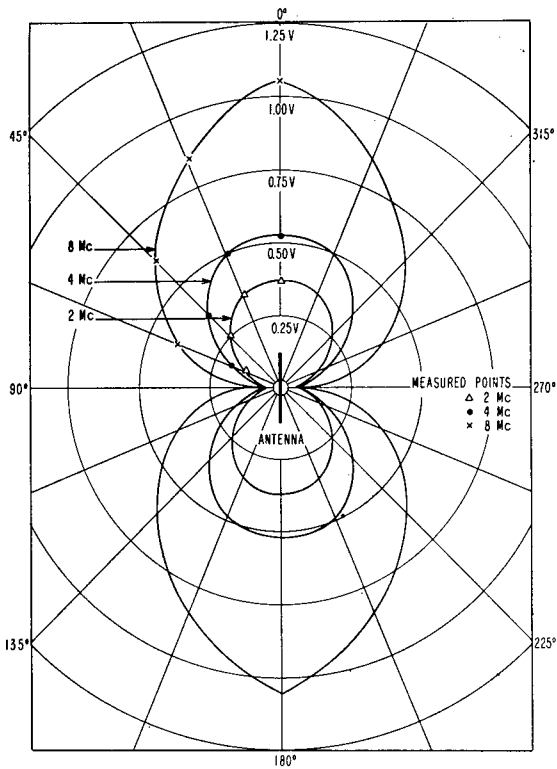
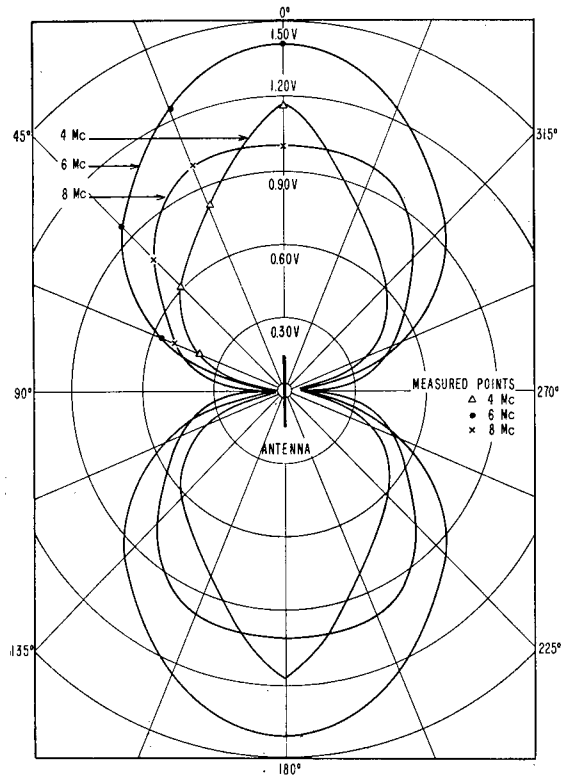


Fig. A-20. Twelve-Foot End-Sealed RG-63/U

SECRET
NAVY-DPPO PRNC, WASH. D.C.

